ELSEVIER

Journal of Chromatography A, 695 (1995) 205–221

JOURNAL OF CHROMATOGRAPHY A

Selectivity due to conformational differences between helical and non-helical peptides in reversed-phase chromatography

T.J. Sereda*, C.T. Mant, R.S. Hodges

Department of Biochemistry and the Medical Research Council of Canada Group in Protein Structure and Function, University of Alberta, Edmonton, Alberta T6G 2H7, Canada

First received 9 August 1994; revised manuscript received 17 November 1994; accepted 18 November 1994

Abstract

The reversed-phase retention behaviour of two series of peptides, one non-helical and the other α-helical, was studied under various linear AB gradients in order to determine the effect of peptide conformation on selectivity of the separation. The non-helical series, designated X1, with the sequence Ac-XLGAKGAGVG-amide, exhibited negligible α-helical content in a hydrophobic medium; whereas, the amphipathic α-helical series, designated AX9, with the sequence Ac-EAEKAAKEXEKAAKEAEK-amide, exhibited high α-helical content in a hydrophobic medium. We have shown that plots of $\log \bar{k}$ vs. $\bar{\phi}$ (where $\bar{k}$ is the median capacity factor and $\bar{\phi}$ is the median volume fraction of organic solvent) are very similar for any one peptide conformation, i.e., peptides from either the non-helical or amphipathic α-helical series exhibit similar S (solute parameter) values and the b (gradient steepness parameter) values are also similar for 17 different amino acid substitutions within each series of peptides. If mixtures of peptides from the two different series are separated using either increasing or decreasing gradient rates, large increases in resolution occur due to selectivity, which may be attributed to the difference in the $\log \bar{k}$ vs. $\bar{\phi}$ plots for each series of peptides. In addition, by using a polymer of an X1 peptide, which is 20 residues in length, it has been shown that the molecular mass difference between the X1 and the AX9 series of peptides is not sufficient to account for the selectivity difference. The S value of a non-amphipathic α-helical peptide further suggested that the difference in selectivity between the two series of peptides was due to differences in conformation. We believe that the peptide mixtures presented here provide a good model for studying selectivity effects due to conformational differences between peptides, an important concern when attempting to develop rational approaches to the prediction and optimization of peptide separation protocols from primary sequence information alone.

1. Introduction

The emergence over the past decade of reversed-phase chromatography (RPC) as the most widely used mode of high-performance liquid chromatography (HPLC) [1] has also seen a concomitant interest in method development protocols to maximise the excellent resolving power of this technique [2–6]. Indeed, this laboratory has been active for several years in developing empirical approaches to correlate the reversed-phase retention behaviour of peptides during linear gradient elution. This work has focused in two major areas: (1) prediction of peptide retention times during RPC from sequence information alone, based on the assignment of a specific hydrophobicity value to each amino acid side chain [7–9]; (2) prediction of the

* Corresponding author.

0021-9673/95/$09.50
SSDI 0021-9673(94)01147-8

effect of varying mobile phase components (e.g., ion-pairing reagent) [10] or run conditions (gradient-rate, flow-rate) [11] on peptide separations. From such studies, we are able to predict, with considerable accuracy, how manipulation of the mobile phase or run conditions will affect the selectivity (and, hence, resolution) of a particular peptide separation. These predictive approaches both rely on relating the predicted retention times of peptides of interest to that of the observed behaviour of a peptide standard [7–11]. This approach to the optimization of peptide resolution assumes that, when not subject to conformational restraints, the chromatographic behaviour of a peptide is mainly or solely dependent on amino acid composition. When one also takes into account the effect of peptide chain length, also independent of any conformational considerations, this assumption holds up well for most practical purposes, as evidenced by the successful use of a computer-based HPLC method development program, ProDigest-LC, derived from these principles [3,12].

It is well known that the general rule of thumb whereby it is assumed that the resolution between all peaks in a peptide mixture will increase with increased gradient time is not necessarily valid [5]. Indeed, variation of selectivity with gradient slope is commonly observed for peptides and proteins [13–18]. A very important, practical example is the occasional reversal of elution order of peptides when attempting to optimize the separation of peptide fragments from a protein digest [13], i.e., different peptides are affected to a different extent by changes in gradient slope. These selectivity variations arise from the way an individual peptide interacts with the hydrophobic stationary phase, a factor not taken into account in a purely empirical approach to prediction and optimization of peptide retention behaviour. Clearly, to enhance the value of such empirically derived predictive methods even further, it is necessary to take into account more stringently the way individual peptide solutes interact with a reversed-phase packing, i.e., a form of fine-tuning of predictions derived solely from the knowledge of peptide primary structure information. A prime resource for such fine-tuning is represented by the *linear solvent strength (LSS)* theory of gradient elution [19–23], which enables the researcher to assign parameters to peptidic solutes reflecting differences in both the magnitude and overall affinity of the hydrophobic contact area between the peptide and the hydrophobic stationary phase. The practical value of LSS theory has already been demonstrated by its application in the development of the DryLab HPLC optimization program [2,4,24].

Clearly, many and varied influences will impact on the way a particular peptide will interact with a reversed-phase packing. These will include characteristics of the peptide itself, e.g., amino acid composition [7,9], residue sequence [9,25,26], peptide length [8] and the presence of any secondary structure (α-helix or β-sheet) which will affect profoundly the way in which residues are orientated with respect to the stationary phase [9,27]; mobile phase (e.g., type of organic modifier, ion-pairing reagent, pH) [1,10,28,29] and run conditions (e.g., temperature) [28–30] make their own contribution to peptide chromatographic behaviour; finally, the effect of the stationary phase (e.g., type of ligand, ligand density, silica- versus non-silica-based) must also be considered [31,32]. In order to delineate the relative contribution of different peptide characteristics to its orientation with a reversed-phase packing, it is necessary to reduce as much as possible the number of variables which affect its retention behaviour.

The present study represents our initial investigation into how the presence of a defined structure (α-helix) affects the magnitude of the contact area of a peptide with a hydrophobic stationary phase, as expressed by LSS theory, and how this effect relates to selectivity differences between families of secondary structure (amphipathic versus non-amphipathic α-helices) as well as to differences between such structures and peptides with no ordered higher levels of structure (random coil). The importance of gauging the contribution of α-helical structure to the selectivity of peptide separations can be easily appreciated in such aforementioned applications as optimization of the separation of peptide

fragment mixtures from chemical or proteolytic digests of proteins; such mixtures typically contain peptides with α-helical potential. Thus, in the present study, RPC was applied, under defined mobile phase and run conditions, to linear gradient elution of series of synthetic model α-helical and non-helical peptides on an analytical reversed-phase column. We believed that observation of the retention behaviour of such peptide models would offer insight into the way such structures affect separation selectivity and, hence, how such information may be applied to the rational development of separation prediction and optimization protocols.

2. Experimental

2.1. Materials

HPLC-grade water and acetonitrile were obtained from BDH (Poole, UK). ACS-grade orthophosphoric acid was obtained from Anachemia (Toronto, Canada). Trifluoroethanol (TFE) was obtained from Sigma (St. Louis, MO, USA).

2.2. Instrumentation

Peptide synthesis was carried out on an Applied Biosystems peptide synthesizer Model 430 (Foster City, CA, USA). Crude peptides were purified by RPC using an Applied Biosystems 400 solvent delivery system connected to a 783A programmable absorbance detector.

The analytical HPLC system consisted of an HP1090 liquid chromatograph (Hewlett-Packard, Avondale, PA, USA), coupled to an HP 1040A detection system, HP9000 series 300 computer, HP9133 disc drive, HP2225A Thinkjet printer and HP7460A plotter.

Amino acid analyses of purified peptides were carried out on a Beckman Model 6300 amino acid analyser (Beckman Instruments, Fullerton, CA, USA).

The correct primary ion molecular masses of peptides were confirmed by time of flight mass spectroscopy on a BIOION-20 Nordic (Uppsala, Sweden).

2.3. Peptide synthesis

Peptides were synthesized by the solid-phase technique (SPPS) on co-poly(styrene–1% divinylbenzene) benzhydrylamine hydrochloride resin (0.92 mmol of amino groups/g resin) as described previously [33]. The cleaved peptide/resin mixtures were washed with diethylether (3×25 ml) and the peptides extracted with neat acetic acid (3×25 ml). The resulting peptide solutions were then lyophilized prior to purification.

2.4. Columns and HPLC conditions

Crude peptides were purified on a semi-preparative SynChropak RP-P C_{18} reversed-phase column (250×10 mm I.D., 6.5 μm particle size, 300 Å pore size) from SynChrom (Lafayette, IN, USA). The peptides were purified at pH 2 by linear AB gradient elution (0.5% B/min) at a flow-rate of 5 ml/min, where eluent A is 0.1% aqueous trifluoroacetic acid (TFA) and eluent B is 0.1% TFA in acetonitrile.

Analytical runs were carried out at pH 2 on an Aquapore RP-300 C_8 reversed-phase column (220×4.6 mm I.D., 7 μm particle size, 300 Å pore size) from Applied Biosystems, by employing linear AB gradient elution (0.5, 1, 2, 4% acetonitrile/min) at a flow-rate of 1 ml/min, where eluent A is 20 m*M* aqueous phosphoric acid and eluent B is 20 m*M* phosphoric acid in 50% aqueous acetonitrile.

2.5. Circular dichroism (CD) measurements

CD measurements were performed on a Jasco J-720 spectropolarimeter (Jasco, Easton, MD, USA). The cell was maintained at 25°C with a Lauda RMS circulating water bath (Lauda, Westbury, NY, USA). The instrument was routinely calibrated with *d*(+)-10-camphorsulphonic acid at 290.5 nm and with pantoyllactone at 219 nm by following the procedures outlined by the manufacturer. CD spectra were the average of

10 scans obtained by collecting data from 250 to 190 nm. The molar ellipticity is reported as mean residue molar ellipticity ($[\theta]$, with units of deg · cm^2/dmol) and calculated from the following equation: $[\theta] = [\theta]_{obs}\ (mrw)/10lc$, where $[\theta]_{obs}$ is the observed ellipticity in degrees, *mrw* is the mean residue weight (molecular mass of the peptide divided by the number of amino acid residues), c is the peptide concentration in g/ml and l is the optical path length in cm (0.0195 cm). Peptide concentrations were determined by amino acid analysis where the stock solution of the "native" model amphipathic α-helical peptide, designated AA9 (see Section 4.1.), was determined to be 5.62×10^{-4} *M* and that of a non-amphipathic α-helical peptide, designated naA, was determined as 1.99×10^{-4} *M*. CD spectra were measured of peptides dissolved in 40 m*M* aqueous phosphoric acid–TFE (1:1, v/v), where TFE is a solvent that induces helicity in single-chain potentially α-helical peptides [34,35].

3. Theoretical considerations

The LSS model describing mathematically the retention behaviour of solutes under gradient elution conditions has been reported in detail elsewhere [19–23] and only the appropriate equations used will be discussed here.

An important quantity in LSS theory is the gradient steepness parameter, b, which is a function of the separation conditions, e.g., the gradient time, flow-rate and mobile phase composition. The retention times of a peptide, t_{g1} and t_{g2}, obtained under two different gradient times, t_{G1} and t_{G2}, may be used to determine the gradient steepness parameter through the following expression:

$$b = t_0 \log \beta / \left[t_{g1} - (t_{g2}/\beta) + t_0'(t_{G1} - t_{G2})/t_{G2}\right] \quad (1)$$

where β is the ratio of gradient times, t_{G2}/t_{G1}, t_0 is the column dead time and t_0' is the column dead time plus the gradient elapse time (gradient elapse time = t_d, time it takes a change in mobile phase composition to move from the pump through the mixer and injector to the column inlet). The t_0 value, in min, was obtained by injecting a sample containing 1% TFA with the column in place [36]. The gradient elapse time was obtained by removing the column and measuring the time for the gradient to reach the detector when a switch from 0 to 50% B is made [36]. The t_0' value was calculated as the column dead time (t_0) plus the gradient elapse time (t_d). For our HPLC system, $t_0' = 3.73$ min and $t_0 = 2.83$ min.

Once a b value has been obtained, the median capacity factor, $\bar{k}$, (i.e., the capacity factor when the solute is at the midpoint of the column during a gradient run) and the median volume fraction of organic solvent, $\bar{\phi}$ (i.e., the volume fraction of organic solvent when the solute is at the midpoint of the column during a gradient run) associated with the elution of each peptide may be determined from the following relationships:

$$\bar{k} = 1/1.15b \quad (2)$$

$$\bar{\phi} = \phi_0 + \left[t_{g1} - t_0' - 0.3(t_0/b)\right](\Delta\phi/t_{G1}) \quad (3)$$

where $\Delta\phi = (\phi_f - \phi_0)$ and ϕ_0 is the initial value at time zero and ϕ_f is the final value, i.e., at the end of the gradient. It has been stated that, in order to optimize a particular separation, the $\log \bar{k}$ value should be within a narrow range of values, i.e., $0 \leq \log \bar{k} \leq 1$ [19,20]. It should be noted that the four different gradient rates used in this study for the separation of the synthetic peptides result in a $\log \bar{k}$ value that approximates this range of values. The $\bar{k}$ and $\bar{\phi}$ values obtained from Eqs. 2 and 3 may be related through the following expression:

$$\log \bar{k} = \log k_0 - S\bar{\phi} \quad (4)$$

Linear plots of $\log \bar{k}$ versus $\bar{\phi}$ were obtained in each case over the experimental range of conditions used and the reported S and $\log k_0$ values were obtained by analysing these data by linear regression. The parameters S and $\log k_0$ are related respectively to the hydrophobic contact area of the peptide and the affinity of this contact region for the hydrophobic stationary phase [18].

Although, strictly speaking, system-to-system consistency requires that solute resolution under gradient conditions requires a calculation that is different from isocratic conditions [19], for the sake of simplicity we have used the isocratic form of the equation to report resolution: $R_s = 1.176\Delta t/(w_{h1} + w_{h2})$, where Δt is the difference in retention time between the two peaks and w_{h1} and w_{h2} are the widths of the peaks at half height for the corresponding peaks [36].

4. Results and discussion

4.1. Design of model synthetic peptides

The suggestion that the solute parameter, S, is dependent on conformation, e.g., random coil versus ordered or native versus denatured has been considered previously [20]. For instance, in an attempt to determine the relationship between structure and the solute parameter, the S values of synthetic peptides of human growth hormone (hGH) were determined [37]; in another study [38], variations in S values of the peptides bombesin, β-endorphin and glucagon with increasing temperature were followed and related to temperature-induced conformational changes. Other studies produced observations that S values may vary considerably for series of peptides which differ markedly in length and sequence [22,39]; whilst only small S value variations were observed for minor changes in the sequence of peptide analogues of myosin light chain [40]. In these latter studies, the conformation of the peptides was not specifically defined or related to the resulting S values.

We believed the best initial approach to delineating the effect of α-helical structure on the solute parameter was to compare the retention behaviour of peptides with extremes of structure, i.e., either with as close to 100% α-helical conformation as possible or with the complete absence of α-helix. To this end, two series of peptides designed to exhibit markedly different conformational characteristics during RPC were synthesized, the sequences of which are shown in Fig. 1.

The peptide series designed to exhibit negligible α-helical structure (denoted X1 in Fig. 1), has the sequence Ac-Xxx-Leu-Gly-Ala-Lys-Gly-Ala-Gly-Val-Gly-amide, where Xxx represents the amino acid substituted at position 1; thus, G1 represents a 10-residue peptide with a glycine residue substituted at position 1. Based on the same sequence as peptide G1, the peptide designated $(G1)_2$, a 20-residue peptide (Fig. 1), was also synthesized in order to determine any molecular mass (or chain length) effect on the S value.

The second series of peptides, denoted AX9 (Fig. 1), has the sequence Ac-Glu-Ala-Glu-Lys-Ala-Ala-Lys-Glu-Xxx-Glu-Lys-Ala-Ala-Lys-Glu-Ala-Glu-Lys-amide, where Xxx represents the substituted position, a sequence known to have a high potential to form an α-helix, specifically an amphipathic α-helix [41,42]. In a similar manner to the designation of the X1 series of peptides, the analogues of this second series are identified by the substituted residue; thus, the designation AA9 refers to an alanine residue substitution at position 9 of the sequence, etc. An additional peptide, designated naA (Fig. 1), with the same composition as peptide AA9 but a different sequence was also synthesized. This peptide, also with high α-helical potential, represents a non-amphipathic α-helical control peptide to assess any effect of amphipathicity, as opposed to strictly α-helical conformational influences, on the S value of an α-helical peptide.

4.2. Conformation and helicity of model peptides

Conformation of the peptides was determined by CD in aqueous solution in the presence of 50% (v/v) TFE. As noted above, this solvent promotes helix formation only in regions of a polypeptide with some helical propensity [34,43–45]. This concentration of TFE is also a good mimic of the hydrophobic environment of RPC, known to induce and stabilize α-helical structure in potentially helical molecules [9].

It has been shown previously by Zhou et al. [9] that the sequence of the peptide series denoted X1 (Fig. 1) exhibits the desired negli-

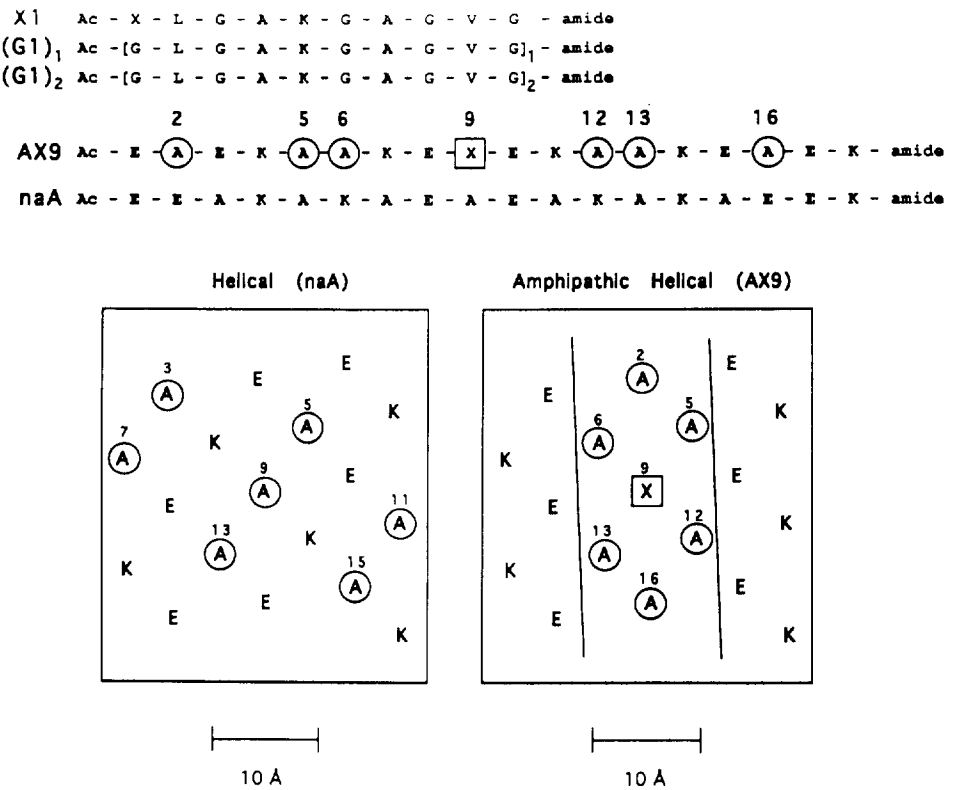

Fig. 1. Design of synthetic peptides. Top: sequence of the non-helical peptide analogues, denoted X1, the amphipathic α-helical peptides, denoted AX9, and the non-amphipathic α-helical peptide naA. In the X1 series, X refers to the amino acid substituted at position 1 of the 10 residue peptide. In the AX9 series, A represents the amino acid Ala which makes up the hydrophobic face (circled residues labelled 2, 5, 6, 12, 13, and 16) of the α-helical peptide and X refers to the amino acid substituted at position 9 (boxed residue labelled 9) in the α-helical peptide. The Lys (K) and the Glu (E) acid residues make up the hydrophilic face of the helix. The non-amphipathic α-helical peptide, naA, is of the same sequence as the AA9 peptide, except that the amino acid sequence is different such that the Ala residues are not all in the hydrophobic face as in peptide AA9. Bottom: Non-amphipathic α-helical and amphipathic α-helical peptides are represented as α-helical nets. The position of the α-carbon atom for each amino acid residue is denoted on the surface of a cylinder representing the α-helix having 3.6 residues per turn, with a 1.5 Å translation along the helix and a helix axis of 5 Å. This cylindrical surface area is depicted in two dimensions where the width of the α-helical net represents the circumference of the cylinder ($2\pi r = 31.4$ Å). The area between the solid lines of the amphipathic α-helical net represents the residues that are in the hydrophobic face of the peptide. In the naA peptide, it can be seen that the distribution of the Ala residues results in a non-amphipathic structure.

gible α-helical structure required for the present study.

Both peptides AA9 and naA exhibit CD spectra typical of α-helical proteins, with two minima at 222 and 207 nm [46] with α-helical contents exceeding 90% at 5°C using the molar ellipticity at 222 nm [41]. In addition, the $[\theta]_{220}/[\theta]_{207}$ ratio value is less than 1, suggesting that, in the presence of 50% TFE, peptides AA9 and naA are single-stranded α-helices [41,47,48]. It has been shown previously [49] that even 29- and 36-residue synthetic amphipathic α-helical peptides which form very stable coiled-coil structures are chromatographed as monomers during size exclusion HPLC in 0.1% aq. TFA containing 50% TFE. Taken together, these observations suggest that peptide AA9, as well as the non-amphipathic naA, will be chromatographed as a single-stranded α-helix during RPC.

4.3. RPC retention behaviour of amphipathic versus non-amphipathic α-helical peptides

Fig. 1 also shows the structures of the amphipathic α-helical series of peptides, AX9, and the non-amphipathic naA presented as α-helical nets. The amphipathic nature of the AX9 series is quite clear, with the circled alanine residues at positions 2, 5, 6, 12, 13 and 16 and the substituted residue at position 9 making up the hydrophobic face of the peptide. The orientation of hydrophobic residues along a helix in such a manner also gives rise to a preferred binding domain in RPC, whereby the observed peptide retention time is greater than would be expected from predictions based on sequence and chain length information alone [9,50]. In contrast, the helical net presentation of peptide naA, which has the same amino acid composition as peptide AA9, demonstrates a distribution of alanine residues throughout the helix, such that no preferred binding domain is formed; hence, naA would be expected to be eluted prior to AA9 from an RPC column [9,50].

4.4. Selectivity differences between non-helical and amphipathic α-helical peptides

Four analogues of the non-helical peptide series (peptides A1, L1, Y1 and F1) and four analogues of the amphipathic α-helical series (peptides AA9, AL9, AY9 and AF9) were run on a reversed-phase column at different linear gradient rates of 0.5%, 1%, 2% and 4% acetonitrile/min. From these data, the median capacity factor, $\bar{k}$, was calculated using Eqs. 1 and 2 and the median volume fraction, $\bar{\phi}$, was calculated using Eq. 3, as described in the Experimental section. Figs. 2, 3 and 4 show plots of $\log \bar{k}$ versus $\bar{\phi}$ for selected pairs of non-helical and amphipathic α-helical peptides; S and $\log k_0$ values subsequently obtained from these plots are reported in Table 1.

From Table 1, it can be seen that the S values

Table 1
Retention time, S and $\log k_0$ values of non-helical and amphipathic α-helical peptides

	t_R (min)[b]				S[c]	$\log k_0$[c]
t_G (min)[a]	100	50	25	12.5		
Gradient rate (%)[a]	0.5	1	2	4		
Helical peptides[d]						
naA	30.10	17.79	11.19	7.70	33.2	4.34
AA9	39.65	22.72	13.77	9.04	27.2	4.93
AL9	48.15	27.06	16.06	10.20	24.1	5.44
AY9	40.25	23.04	14.02	9.18	24.9	4.62
AF9	47.25	26.60	15.90	10.12	23.4	5.20
Non-helical peptides[d]						
$(G1)_1$	21.85	14.73	10.34	7.66	13.2	1.53
$(G1)_2$	34.69	20.70	13.09	8.87	17.4	2.91
A1	23.47	15.61	10.80	7.90	13.0	1.63
L1	35.25	21.89	14.16	9.67	11.1	2.17
Y1	31.37	19.66	12.91	8.97	12.3	2.07
F1	38.13	23.35	14.93	10.12	10.5	2.24

[a] t_G represents the length of the linear AB gradient, in min, for a change from 0 to 100% B and the rate represents the equivalent % acetonitrile/min for the corresponding gradient time. For conditions, see Experimental.
[b] t_g represents the retention time of each peptide under linear AB gradient conditions.
[c] S and $\log k_0$ are determined by linear regression of the data from the $\log \bar{k}$ vs. $\bar{\phi}$ as described by Synder and Stadalius [20]; see Experimental.
[d] For details of peptide designations, see Section 4.1. and Fig. 1.

obtained for the non-helical and amphipathic α-helical peptides represent a small range of values within each series of peptides (i.e., 10.5 to 13.0 and 23.4 to 27.2, respectively); in contrast, there is a significant difference in S values between the two series of peptides. According to Snyder [19], the separation of solutes of different S values may result in three different types of $\log \bar{k}$ vs. $\bar{\phi}$ plots; in addition, it is also suggested by Snyder and Stadalius [20] that any condition that affects the value of $\bar{k}$ (e.g., the gradient time, t_G) will result in a change in $\bar{\phi}$, this change in $\bar{\phi}$ subsequently resulting in a change in selectivity. Aguilar et al. [39] and Hearn et al. [15] also suggest that selectivity differences between polypeptides will be related to their respective S values.

The elution profiles shown in Figs. 2, 3 and 4, where selected pairs of peptides (each pair including one peptide from each peptide series) are separated under different gradient conditions, represent excellent practical examples of the three types of $\log \bar{k}$ vs. $\bar{\phi}$ plot discussed by Snyder [19]. Thus, very different effects of varying gradient rate on the selectivity of the separation of the peptide pairs are observed in Figs. 2–4.

From Fig. 2 (left), it can be seen that the non-helical peptide, L1, and the amphipathic α-helical peptide, AY9, have the same median capacity factor at a gradient rate of 1.8% acetonitrile/min, i.e., the point where the two plots intersect; thus, the two peptides are coeluted, as seen in Fig. 2 (right), panel B. Since the plots of the two peptides intersect at a point in the centre of the workable range of median capacity factor, i.e., where peptide retention times are neither too short nor too long for practical purposes, separation of the two peptides may be achieved either by decreasing the gradient rate (the more traditional approach) [Fig. 2 (right), panel A], or increasing the gradient rate (panel C) [19]. Thus, by decreasing the gradient rate from 1.8% acetonitrile/min (panel B) to 0.5%/min (panel A), peptides L1 and AY9 were separated by 5 min (from Table 1: AY9, $t_g = 40.25$ min; L1, $t_g = 35.25$ min). Alternatively, by increasing the gradient rate from 1.8%/min (panel B) to 4%/min (panel C), peptides L1 and AY9 are separated by 0.49 min (Table 1: L1, $t_g = 9.67$ min; AY9, $t_g = 9.18$ min). Note the reversal of peptide elution order between the two extremes of gradient rate, a consequence of the intersecting plots shown in Fig. 2 (left) and an excellent example of changes in separation selectivity due to significantly different peptide S values [13,17].

Fig. 3 represents a second type of $\log \bar{k}$ vs. $\bar{\phi}$ plot [19], where the lines for the two peptides intersect at the higher end of practically favourable median capacity factors. Thus, at a gradient rate of 0.77% acetonitrile/min, the median capacity factor for the non-helical/amphipathic α-helical peptide pair F1/AA9 is the same (Fig. 3, left); therefore, there is no separation selectivity and the peptides are coeluted [Fig. 3 (right), panel A]. Again in this case, the peptide S values are substantially different (Table 1: AA9, $S = 27.2$ and F1, $S = 10.5$) and a change in selectivity may be achieved by varying the gradient rate [19]. For this peptide pair, the best option clearly is to increase the gradient to separate the peptides within a reasonable run time. Thus, the separation improved progressively as the gradient rate was increased from 0.77% acetonitrile/min (panel A) to 1%/min (panel B) and, finally, to 4%/min (panel C). In addition, this separation was achieved within a short run time (< 10 min) and resulted in sharp solute peaks.

Fig. 4 shows the separation of the peptide pair L1/AL9, which also exhibit significantly different S values (Table 1: L1, $S = 11.1$ and AL9, $S = 24.1$). These peptides produce the third type of $\log \bar{k}$ vs. $\bar{\phi}$ plot [19], where the individual peptide plots intersect at the lower end of the practical working range of $\log \bar{k}$ values. Clearly, for this peptide pair, a decreasing gradient rate would be the appropriate method to improve the separation. Thus, decreasing the gradient rate from 4% acetonitrile/min [Fig. 4 (right), panel C] to 2%/min (panel B) and, finally to 0.5% acetonitrile/min (panel A) results in a progressive improvement in peptide separation; at a gradient rate of 0.5% acetonitrile/min, the peptides are separated by 12.90 min (Table 1: AL9, $t_g = 48.15$; L1, $t_g = 35.25$).

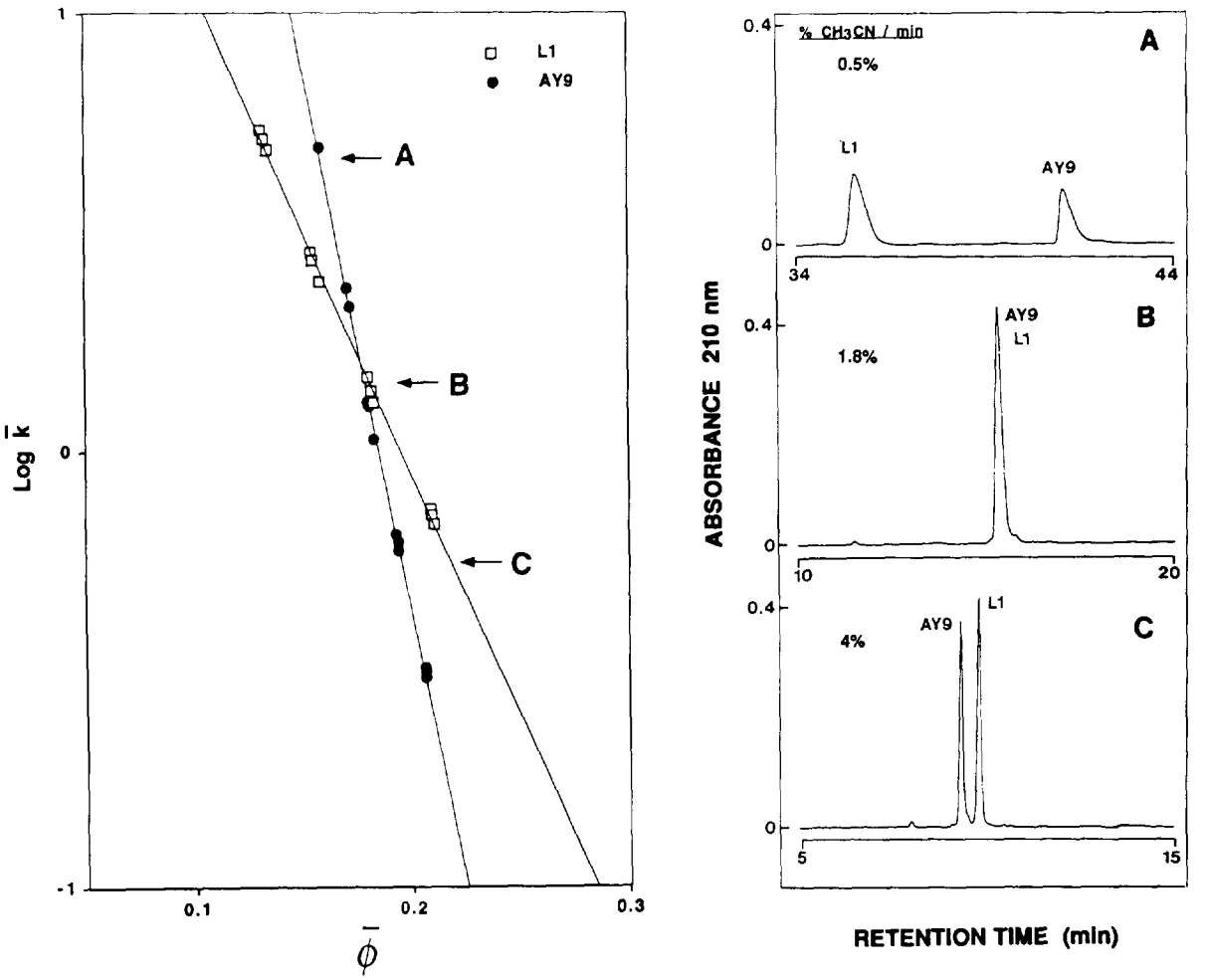

Fig. 2. Plot of log $\bar{k}$ vs. $\bar{\phi}$ and reversed-phase elution profiles of peptides L1 and AY9. Plot: values of log $\bar{k}$ and $\bar{\phi}$ were obtained by separating L1 and AY9 at four different gradient rates (see Table 1) and applying Eqs. 1, 2 and 3 to the retention time data as described in Experimental. Straight line plots were obtained by linear regression of the data. The labels A, B and C refer to the elution profiles shown in the right hand panels. RPC: peptides L1 and AY9 were separated at 0.5, 1.8 and 4% acetonitrile/min at a flow-rate of 1 ml/min where eluent A was 20 m*M* phosphoric acid and eluent B was 20 m*M* phosphoric acid in 50% aqueous acetonitrile.

4.5. Contribution of conformational differences to selectivity of peptide separations

We now set out to determine the role that conformation played in the selectivity differences apparent between the non-helical and amphipathic α-helical peptides demonstrated in Figs. 2–4 and Table 1. The peptide pairs of Figs. 2–4 not only differed in conformation (non-helical X1 series versus α-helical AX9 series), but also in molecular mass (or polypeptide chain length) (10-residue X1 series versus 18-residue AX9 series). Thus, it was now necessary to determine the contribution, if any, of hydrophobicity and molecular mass to the magnitude of the *S* values obtained for the two series of peptides in order to delineate the effect of α-helical conformation on separation selectivity.

Despite the significant range of hydrophobicities of the non-helical X1 series of peptides,

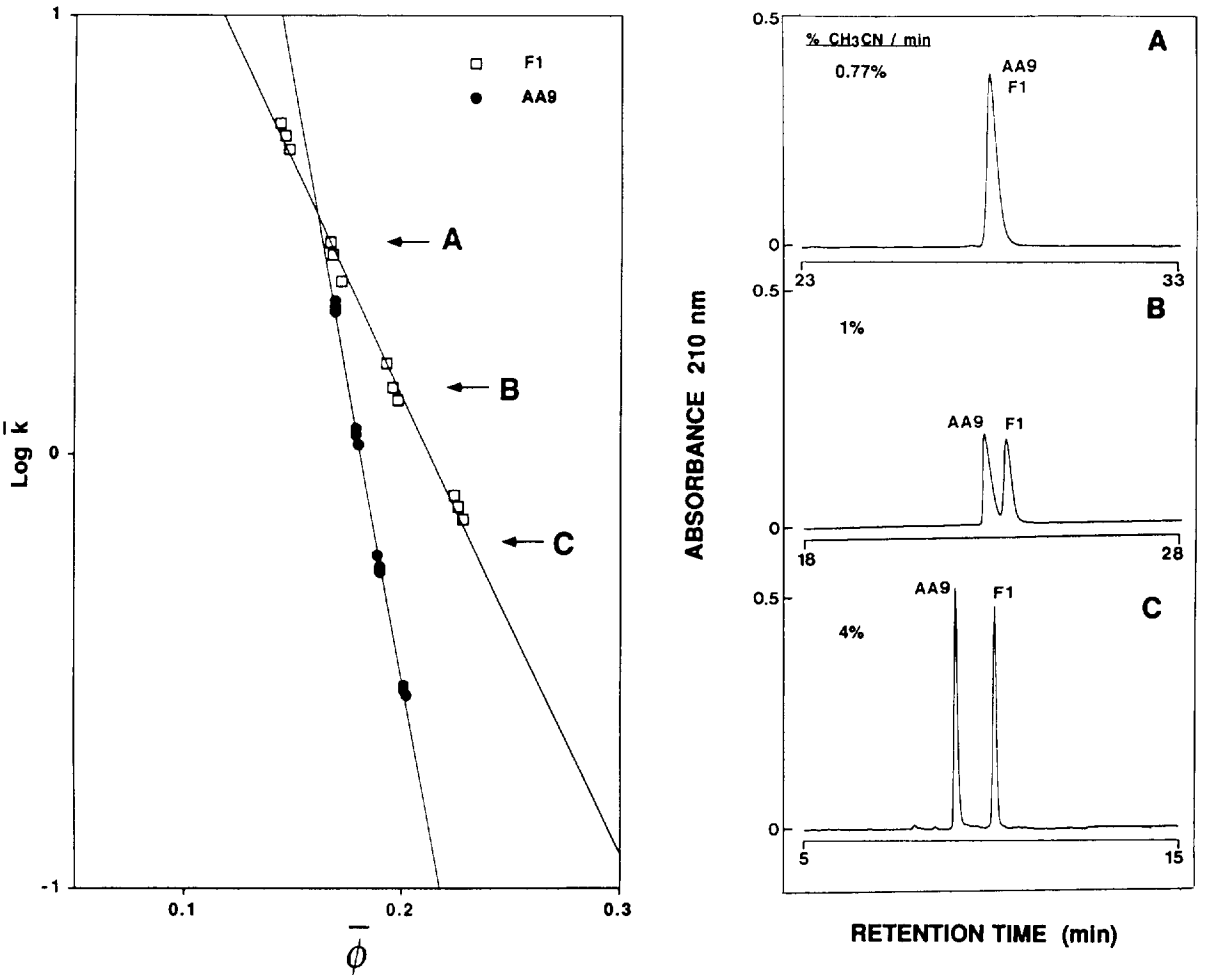

Fig. 3. Plot of $\log \bar{k}$ vs. $\bar{\phi}$ and reversed-phase elution profiles of peptides F1 and AA9. Plot: obtained as in Fig. 2. RPC: conditions as in Fig. 2, except that gradient rates of 0.77, 1.0 and 4% acetonitrile/min were used.

as expressed by their retention times (23.47 to 38.13 min at 0.5% acetonitrile/min; Table 1), the corresponding range of S values was relatively small (10.5 to 13.0; Table 1); similar observations were made for the amphipathic α-helical AX9 series of peptides where the retention times varied from 39.65 to 48.15 min with a small S value range of 23.4 to 27.2 (Table 1).

It has been observed that S is dependent on molecular mass; however, it has been found that this relationship is very much dependent on the peptides used in the determination [40]. It has therefore been suggested [22] that it is not the molecular mass per se that is important in determining S.

From Fig. 1, non-helical peptides $(G1)_1$ and $(G1)_2$ were now chromatographed at different gradient rates and their S values calculated from plots of $\log \bar{k}$ vs. $\bar{\phi}$. Peptide $(G1)_1$ is the glycine-substituted 10-residue analogue of the X1 peptide series; whereas, $(G1)_2$ is a 20-residue polymer of $(G1)_1$ and represents a non-helical control peptide similar in length to the 18-residue

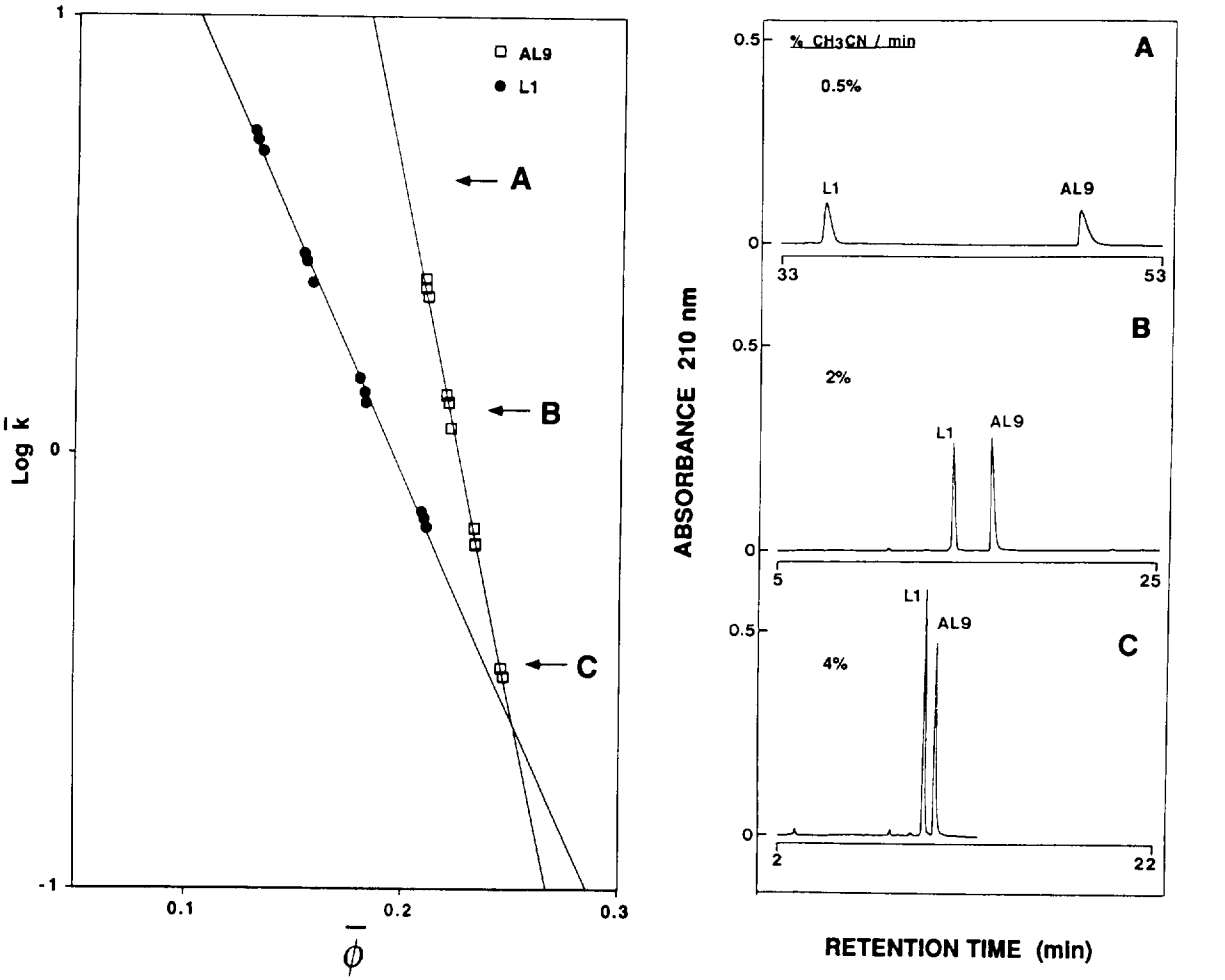

Fig. 4. Plot of $\log \bar{k}$ vs. $\bar{\phi}$ and reversed-phase elution profiles of peptides L1 and AL9. Plot: obtained as in Fig. 2. RPC: conditions as in Fig. 2, except that gradient rates of 0.5, 2.0 and 4% acetonitrile/min were used.

α-helical series of peptides (AX9). From Table 1, the $(G1)_1$ peptide has an S value (13.2) that is similar to the range of values determined for other non-helical 10-residue peptides, A1, L1, Y1 and F1 (10.5 to 13.0). In addition, it can also be seen that an increase in molecular mass (or chain length) from the 10-residue $(G1)_1$ to the 20-residue $(G1)_2$ ($S = 17.4$), resulted in an increase in S which is consistent with a previous suggestion that the S value may increase with molecular mass through simple peptide elongation [22], as in this example. Thus, although peptide chain length may contribute to some extent, the magnitude of the S value increase observed between the 10-residue and 20-residue peptides (13.2 to 17.4; Table 1) is not large enough to account for the significant differences in the range of S values (and, hence, selectivity differences) between the non-helical 10-residue X1 peptide series ($S = 10.5$ to 13.0; Table 1) and the 18-residue amphipathic α-helical AX9 peptide series ($S = 23.4$ to 27.2; Table 1). Despite the amino acid composition differences between the peptide series, we feel this is strong evidence

that the significantly different S values for the AX9 series of peptides in comparison to the non-helical X1 series is due mainly to the influence of the α-helical conformation of the former.

We now wished to determine whether the amphipathicity had any significant contribution to peptide S values separate from the conformational influence of the helix. The non-amphipathic α-helical peptide, naA (Fig. 1), and the amphipathic α-helical peptide AA9 have hydrophobic moments of 0.04 and 0.59, respectively, determined using the method and normalized consensus hydrophobicity scale of Eisenberg et al. [51]). The hydrophobic moment is a measure of amphipathicity, where the greater the value, the greater the amphipathicity [52]. Peptide naA exhibits a significantly different S value (33.2; Table 1) compared to the non-helical X1 peptides (a range of 10.5 to 13.0; Table 1). Instead, the value for peptide naA is of a magnitude similar to that of its amphipathic analogue, peptide AA9 (27.2; Table 1). Clearly, the amphipathicity of these α-helical peptides is not a major factor influencing peptide S values and, hence, separation selectivity, as compared

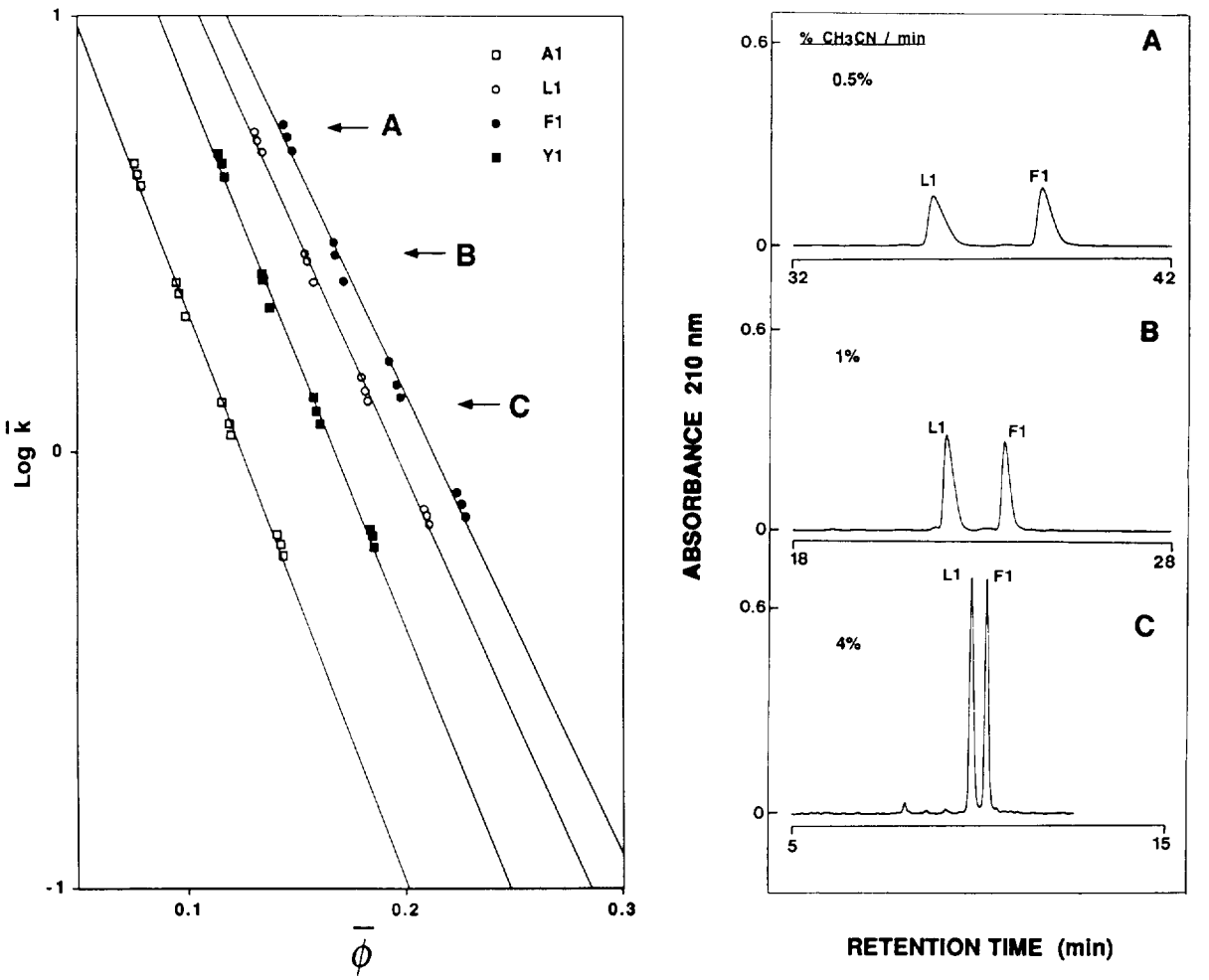

Fig. 5. Plot of $\log \bar{k}$ vs. $\bar{\phi}$ and reversed-phase elution profiles of the non-helical peptides A1, L1, Y1 and F1. Plot: obtained as in Fig. 2. RPC: conditions as in Fig. 2, except that gradient rates 0.5, 1.0 and 4% acetonitrile/min were used.

to the conformational differences between non-helical and helical peptides.

4.6. Resolution between mixtures of non-helical and amphipathic helical peptides

From Figs. 5 and 6, left panels, it can be seen that peptides of similar structure exhibit similar $\log \bar{k}$ vs. $\bar{\phi}$ plots and, therefore, a similar S value; this can also be seen from Table 1, where, as noted above, the non-helical and amphipathic α-helical peptides have a small intra-series range of S values (10.5 to 13.0 and 23.4 to 27.2, respectively). Since S for each series of peptides is represented by a small range of values, this suggests that improvement in resolution between peptides of the same series (and, thus the same conformation) may be obtained by a decreasing gradient rate. Fig. 5 illustrates this situation, where non-helical peptides L1 and F1, having similar values of S (L1 = 11.1 and F1 = 10.5, respectively; Table 1), exhibited a 1.2-fold change in resolution (3.5 to 4.2; Table 2) for a 2-fold (1% acetonitrile/min to 0.5%/min) decrease in gradient rate. Similar results can be seen in Fig. 6, where the two amphipathic α-

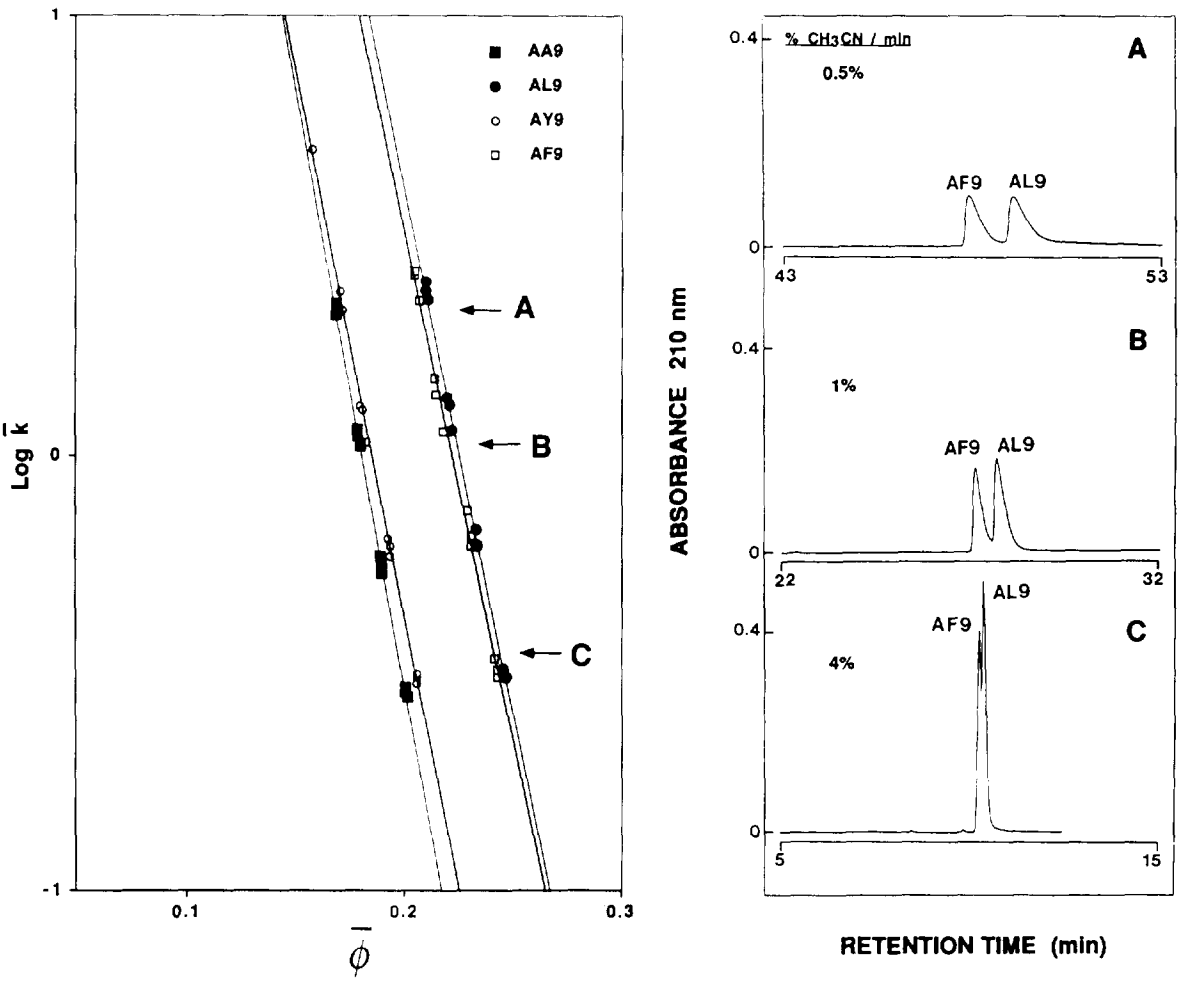

Fig. 6. Plot of $\log \bar{k}$ vs. $\bar{\phi}$ and reversed-phase elution profiles of the amphipathic α-helical peptides AA9, AL9, AY9 and AF9. Plot: obtained as in Fig. 2. RPC: conditions as in Fig. 2, except that gradient rates 0.5, 1.0 and 4% acetonitrile/min were used.

Table 2
Resolution for peptide pairs in Figs. 2–6

Figure[a]	Peptide pair[a]	% Acetonitrile/min[b]	Resolution (R_s)[c]
2	L1/AY9	0.5	7.6
		1.8	0
		4	2.7
3	F1/AA9	0.77	0
		1	1.5
		4	6.1
4	L1/AL9	0.5	17.5
		2	7.2
		4	2.1
5	L1/F1	0.5	4.2
		1	3.5
		4	2.2
6	AF9/AL9	0.5	1.5
		1	1.2
		4	-

[a] Refers to Figs. 2–6 and the corresponding peptide pair separated under the given linear AB gradient conditions (see Experimental for conditions).
[b] % Acetonitrile used for the separation of the reported peptide pair in panels A, B and C, respectively (lowest to highest gradient rate) of Figs. 2–6.
[c] $R_s = 1.176\Delta t/(w_{h1} + w_{h2})$, where Δt is the difference in retention times for the two peaks and w_{h1} and w_{h2} are the widths at half height for each corresponding peak.

helical peptides, AF9 and AL9, exhibited a 1.25-fold change in resolution (1.2 to 1.5; Table 2) for a 2-fold (1%/min to 0.5%/min) decrease in gradient rate.

This is in clear contrast to the situation where changes in selectivity, due to conformational differences between non-helical and amphipathic helical peptides, result in large changes in resolution. For example, in Fig. 2 (right), a decreasing gradient rate results in a large improvement in resolution for the peptide pair L1/AY9; thus, from Table 2, the resolution of this pair increases from 0 to 7.6 for a 3.6-fold decrease in gradient rate (1.8%/min to 0.5% acetonitrile/min). Similarly, in Fig. 4 (right), the resolution of the peptide pair L1/AL9 increases 2.4-fold (7.2 to 17.5; Table 2) for a 4-fold (2%/min to 0.5%/min) decrease in gradient rate. Increasing gradient rates are also shown to improve resolution in Figs. 2 and 3, where an increase in resolution of the peptide pair L1/AY9 (Fig. 2) from 0 to 2.7 (Table 2) is observed for a 2.2-fold (1.8%/min to 4% acetonitrile/min) increase in gradient rate and a 4.1-fold increase in resolution (1.5 to 6.1) of the peptide pair F1/AA9 (Fig. 3) is observed for a 4-fold (1%/min to 4%/min) increase in gradient rate. In these cases, the observed distinct improvements in peptide resolution are likely due solely to changes in selectivity.

Table 3 reports the gradient steepness parameter (b) and median capacity factor ($\bar{k}$) values obtained for 17 analogues of both the non-helical (X1) and α-helical (AX9) series of peptides. The b or $\bar{k}$ within each series of peptides are similar and would exhibit similar plots of $\log \bar{k}$ vs. $\bar{\phi}$ as those shown in Fig. 5 (non-helical peptides) and Fig. 6 (α-helical peptides). This further suggests that within each series of peptides there would only be small changes in selectivity with changes in gradient rate for any mixtures of these peptides. In contrast, there would be a much larger change in resolution of peptides between the two

Table 3
Retention time, gradient steepness parameter and median capacity factor of non-helical and amphipathic α-helical peptides

Amino acid substitution[a]	Helical peptides				Non-helical peptides			
	t_{g1} (min)[b] (2%)	t_{g2} (min)[b] (1%)	b[c]	$\bar{k}$[c]	t_{g1} (min)[b] (2%)	t_{g2} (min)[b] (1%)	b[c]	$\bar{k}$[c]
Ile (I)	16.14	27.13	1.20	0.72	13.72	21.44	0.75	1.16
Leu (L)	16.09	27.20	1.36	0.64	14.08	22.19	0.76	1.14
Phe (F)	15.92	26.78	1.28	0.68	14.83	23.66	0.75	1.16
Trp (W)	15.56	26.23	1.47	0.59	15.24	24.43	0.73	1.18
Val (V)	15.07	25.40	1.69	0.52	12.43	18.91	0.77	1.13
Met (M)	14.88	24.96	1.59	0.55	12.87	19.83	0.78	1.11
Cys (C)	13.97	23.03	1.44	0.60	11.46	16.90	0.74	1.17
Tyr (Y)	13.97	23.20	1.69	0.52	12.70	19.41	0.75	1.15
Ala (A)	13.76	22.81	1.74	0.50	10.66	15.69	0.90	0.97
Thr (T)	12.32	20.00	1.87	0.46	10.52	15.53	0.96	0.91
Glu (E)	12.13	19.77	2.24	0.39	10.73	15.62	0.81	1.08
Gly (G)	11.66	18.77	2.08	0.42	10.27	14.73	0.82	1.06
Ser (S)	11.51	18.36	1.83	0.47	10.12	14.66	0.92	0.94
Asp (D)	11.17	17.67	1.81	0.48	10.43	14.92	0.77	1.13
Gln (Q)	11.17	17.71	1.89	0.46	10.23	14.81	0.89	0.98
Asn (N)	10.14	15.66	1.91	0.45	10.06	14.49	0.90	0.97
Pro (P)	9.94	15.10	1.62	0.54	12.06	18.18	0.77	1.13

[a] Three letter and single letter code represents the amino acid substituted in position 9 of the helical peptide (AX9) or position 1 of the non-helical peptide (X1).
[b] Values between parentheses represent gradient rates. For run conditions, see Experimental.
[c] The gradient steepness parameter, b, and the median capacity factor, $\bar{k}$, are calculated as described by Snyder and Stadalius [20] (see Experimental). For a gradient rate of 2% acetonitrile/min, $t_G = 25$ min; for 1% acetonitrile/min, $t_G = 50$ min.

peptide groups with varying gradient rate due to the large inter-series selectivity differences.

5. Conclusions

In this report we have illustrated the use of two series of synthetic model peptides (non-helical or amphipathic α-helical) in order to demonstrate the selectivity that may be obtained in a reversed-phase separation based on conformational differences between the peptides. Peptides within a series, i.e., non-helical or amphipathic α-helical, exhibit very similar plots of $\log \bar{k}$ versus $\bar{\phi}$ (and, therefore, similar S values), with only small consequent changes in selectivity with changing gradient rate; whereas, peptide mixtures containing peptides from both series of peptides and, hence, containing peptides with large differences in S values, show a correspondingly greater change in separation selectivity with a gradient rate variation. These results are directly applicable to optimizing the separation of mixtures of peptides.

Acknowledgements

This work was supported by the Medical Research Council of Canada Group in Protein Structure and Function and by the Protein Engineering Network of Centres of Excellence program supported by the Government of Canada. We thank Paul Semchuck for synthes-

izing the peptides used in this study and Lorne Burke for technical assistance.

References

[1] C.T. Mant and R.S. Hodges (Editors), *High Performance Liquid Chromatography of Peptides and Proteins: Separation, Analysis and Conformation*, CRC Press, Boca Raton, FL, 1991.

[2] J.W. Dolan and L.R. Snyder, *LC·GC*, 5 (1987) 970.

[3] R.S. Hodges, J.M.R. Parker, C.T. Mant and R.R. Sharma, *J. Chromatogr.*, 458 (1988) 147.

[4] J.L. Glajch and L.R. Snyder (Editors), *Computer-Assisted Method Development for High-Performance Liquid Chromatography*, Elsevier, Amsterdam, 1990.

[5] N. Lundell, *J. Chromatogr.*, 639 (1993) 97.

[6] N. Lundell and K. Markides, *J. Chromatogr.*, 639 (1993) 117.

[7] D. Guo, C.T. Mant, A.K. Taneja, J.M.R. Parker and R.S. Hodges, *J. Chromatogr.*, 359 (1986) 499.

[8] C.T. Mant, T.W.L. Burke, J.A. Black and R.S. Hodges, *J. Chromatogr.*, 458 (1988) 193.

[9] N.E. Zhou, C.T. Mant and R.S. Hodges, *Pept. Res.*, 3 (1990) 8.

[10] D. Guo, C.T. Mant and R.S. Hodges, *J. Chromatogr.*, 386 (1987) 205.

[11] C.T. Mant, T.W.L. Burke, and R.S. Hodges, *LC·GC*, 12 (1994) 396.

[12] C.T. Mant, T.W.L. Burke, N.E. Zhou, J.M.R. Parker and R.S. Hodges, *J. Chromatogr.*, 485 (1989) 365.

[13] J.L. Meek and Z.L. Rossetti, *J. Chromatogr.*, 211 (1981) 15.

[14] J.L. Glajch, M.A. Quarry, J.F. Vasta and L.R. Snyder, *Anal. Chem.*, 58 (1986) 280.

[15] M.T.W. Hearn, M.I. Aguilar, C.T. Mant and R.S. Hodges, *J. Chromatogr.*, 438 (1988) 197.

[16] B.F.D. Ghrist and L.R. Snyder, *J. Chromatogr.*, 459 (1988) 25.

[17] T. Molnar, R. Boysen and P. Jekow, in J.L. Glajch and L.R. Snyder (Editors), *Computer-Assisted Method Development for High Performance Liquid Chromatography*, Elsevier, Amsterdam, 1990, p. 569.

[18] M.I. Aguilar, S. Mougos, J. Boublik, J. Rivier and M.T.W. Hearn, *J. Chromatogr.*, 646 (1993) 53.

[19] L.R. Snyder, in Cs. Horváth (Editor), *High Performance Liquid Chromatography: Advances and Perspectives*, Vol. 1, Academic Press, New York, NY, 1980, p. 207.

[20] L.R. Snyder and M.A. Stadalius, in Cs. Horváth (Editor), *High Performance Liquid Chromatography: Advances and Perspectives*, Vol. 4, Academic Press, New York, NY, 1986, p. 195.

[21] P. Jandera and J. Churácek, *Gradient Elution in Column Liquid Chromatography, Theory and Practice*, Elsevier, Amsterdam, 1985.

[22] M.T.W. Hearn and M.I. Aguilar, *J. Chromatogr.*, 359 (1986) 31.

[23] M.T.W. Hearn, in C.T. Mant and R.S. Hodges (Editors), *High Performance Liquid Chromatography of Peptides and Proteins: Separation, Analysis and Conformation*, CRC Press, Boca Raton, FL, 1991, p. 105.

[24] J.W. Dolan, D.C. Lommen and L.R. Snyder, *J. Chromatogr.*, 485 (1989) 91.

[25] Z. Iskandarini and D.J. Pietrzyk, *Anal. Chem.*, 53 (1981) 489.

[26] R.A. Houghten and S.T. DeGraw, *J. Chromatogr.*, 386 (1987) 489.

[27] M.L. Heinitz, E. Flanigan, R.C. Orlowski and F.E. Regnier, *J. Chromatogr.*, 443 (1988) 229.

[28] W.G. Burton, K.D. Nugent, T.K. Slattery, B.R. Summers and L.R. Snyder, *J. Chromatogr.*, 443 (1988) 363.

[29] K.D. Nugent, W.G. Burton, T.K. Slattery, B.F. Johnson and L.R. Snyder, *J. Chromatogr.*, 443 (1988) 381.

[30] D. Guo, C.T. Mant, A.K. Taneja and R.S. Hodges, *J. Chromatogr.*, 359 (1986) 519.

[31] N.E. Zhou, C.T. Mant, J.J. Kirkland and R.S. Hodges, *J. Chromatogr.*, 548 (1991) 179.

[32] C.T. Mant and R.S. Hodges, in B.L. Karger and W.S. Hancock (Editor), *High Resolution Separation of Biological Macromolecules, Methods in Enzymology*, Academic Press, FL, in press.

[33] T.J. Sereda, C.T. Mant, A.M. Quinn and R.S. Hodges, *J. Chromatogr.*, 646 (1993) 17.

[34] J.W. Nelson and N.R. Kallenbach, *Proteins: Structure, Function and Genetics*, 1 (1986) 211.

[35] J.W. Nelson and N.R. Kallenbach, *Biochemistry*, 28 (1989) 5256.

[36] C.T. Mant and R.S. Hodges, in C.T. Mant and R.S. Hodges (Editors), *HPLC of Peptides and Proteins: Separation, Analysis and Conformation*, CRC Press, Boca Raton, FL, 1991, p. 69.

[37] A.W. Purcell, M.I. Aguilar and M.T.W. Hearn, *J. Chromatogr.*, 476 (1989) 113.

[38] A.W. Purcell, M.I. Aguilar and M.T.W. Hearn, *J. Chromatogr.*, 592 (1992) 103.

[39] M.I. Aguilar, A.N. Hodder and M.T.W. Hearn, *J. Chromatogr.*, 327 (1985) 115.

[40] M.T.W. Hearn and M.I. Aguilar, *J. Chromatogr.*, 392 (1987) 33.

[41] N.E. Zhou, C.M. Kay, B.D. Sykes and R.S. Hodges, *Biochemistry*, 32 (1993) 6190.

[42] N.E. Zhou, O.D. Monera, C.M. Kay and R.S. Hodges, *Protein Peptide Lett.*, in press.

[43] S.R. Lehrman, J.L. Tuls and M. Lund, *Biochemistry*, 29 (1990) 5590.

[44] F. Sönnichsen, J.E. Van Eyk, R.S. Hodges and B.D. Sykes, *Biochemistry*, 31 (1992) 8790.

[45] M. Zhang, T. Yuan and H.J. Vogel, *Protein Science*, 2 (1993) 1931.

[46] Y.-H. Chen, J.T. Yang and H.M. Martinez, *Biochemistry*, 11 (1972) 4120.

[47] N.E. Zhou, C.M. Kay and R.S. Hodges, *J. Mol. Biol.*, 237 (1994) 500.

[48] T.M. Cooper and R.W. Woody, *Biopolymers*, 30 (1990) 657.
[49] S.Y.M. Lau, A.K. Taneja and R.S. Hodges, *J. Chromatogr.*, 317 (1984) 129.
[50] V. Steiner, M. Schär, K.O. Börnsen and M. Mutter, *J. Chromatogr.*, 586 (1991) 43.
[51] D. Eisenberg, E. Schwartz, M. Komaromy and R. Wall, *J. Mol. Biol.*, 179 (1984) 125.
[52] D. Eisenberg, R.M. Weiss and T.C. Terwilliger, *Nature*, 299 (1986) 371.